Determining Tugboat Initial Speed Limit to Avoid Collision with Jetty at Paciran Port

Esqy Dhiya'ul Fuady[1], I Putu Sindhu Asmara[2*], Imam Sutrisno[3]

(Received: 15 July 2025 / Revised: 22 July 2025 /Accepted: 28 July 2025 / Available Online: 5 September 2025)

***Abstract*— Paciran Port experiences growing vessel activity, particularly from limestone barges, highlighting the critical need for safe port operations. Ship berthing inherently carries risks, including potential collisions with the jetty. This study aims to determine the maximum safe initial speed limit for tugboats assisting barge berthing at Paciran Port, to prevent such incidents. We employed a simulation method based on the Maneuvering Modelling Group using MATLAB software. The MMG model considered various environmental factors, including water depth, wind forces, and current effects. The novelty of this paper lies in the integration of the CFD method and MMG to determine hull forces and moments. Hydrodynamic coefficients were obtained from Computational Fluid Dynamics (CFD) analysis and empirical formulas. Berthing speed acceptance criteria were based on PIANC standards. Our simulations, conducted across three environmental conditions and multiple initial speed variations, revealed that an initial speed of 5 knots resulted in "Unfavourable" berthing conditions, increasing collision risk. Conversely, initial speeds below 5 knots consistently allowed for safe berthing, with final speeds remaining below 0.3 m/s, meeting PIANC's Favourable to Moderate criteria. We conclude that the maximum acceptable initial tugboat speed at Paciran Port, to avoid jetty collisions during tugboat-assisted berthing, is below 4 knots.**

Keywords— Maneuvering Modelling Group, MMG, Ship Maneuvering, Barge, MATLAB Simulation.

*Corresponding Author:putusindhu@ppns.ac.id

I. INTRODUCTION

Paciran Port is a critical multipurpose hub in East Java, facilitating domestic sea transport and inter-provincial or inter-regency crossings. The port has seen a notable surge in ship visits and cargo operations, particularly involving barges transporting limestone. This heightened activity necessitates a focus on enhancing port management, services, and infrastructure, while also emphasizing the safety of ship berthing. Given the dynamic nature of ship movements, operators must meticulously manage three key aspects: berthing speed, transverse distance, and closing angle, making adjustments as required to meet specific operational conditions. This ensures the vessel can ultimately achieve a smooth and precise berthing at the designated berth. [1]. Too fast approaches can damage the fender, quay wall, or even impact the hull structure[2].

The process of berthing a ship is inherently risky, often leading to accidents, such as collisions with the jetty, which have been reported in various areas, including Indonesia. While tugboats are crucial for aiding ship maneuvers, operational errors on their part can also contribute to mishaps[3]. Tugboats are crucial for assisting large vessels in confined spaces.

Taimuri assesses the ship's hull hydrodynamic forces, and derivatives are determined using semi-empirical methods, Computational Fluid Dynamics, or model test data[4]. Go and Ahn presented a novel approach to determine the hydrodynamic derivatives of a ship using CFD[5]. Research by Zhao has shown that the Mathematical Maneuvering Model's algorithm is highly accurate, a fact confirmed through simulation experiments[6]. Some Engineers and scientists use MATLAB to solve problems such as simulation experiments on the turning circle and the zigzag maneuvers[7]. Xia reveals that the MMG Model simulated by MATLAB obtains a result that broadly aligns with the actual condition[8].

The main advantage of the MMG (Maneuvering Model Group) mathematical model is its ability to simulate ship maneuvering motions with high precision in various complex situations[9]. The MMG Model is calculated by considering environmental disturbances such as water depth, wind force and moment, and current effect[10]. This research will employ a simulation method based on the Maneuvering Modelling Group, utilizing the MATLAB program, to analyze the safety of the barge berthing process at Paciran Port. MMG simulation is capable of evaluating the ability of tugboats in assisting berthing and unberthing, and also assessing the possibility of collisions[11].

This Paper aims to determine the tugboat's initial speed limit to avoid collision between the barge and jetty during the berthing process. The PIANC Standard is used to determine safe speed limits when berthing.

II. METHOD

A. The 3 DOF motion equations

The equations (1) to (3) express the motion of surging, swaying, and yawing of vessels[12].

Esqy Dhiya'ul Fuady is with Departement of Safety and Risk Engineering, Surabaya State Shipbuilding Polytechnic, Surabaya, 60111, Indonesia. esqyfuady@student.ppns.ac.id

I Putu Sindhu Asmara is with Departement of Safety and Risk Engineering, Surabaya State Shipbuilding Polytechnic, Surabaya, 60111, Indonesia. putusindhu@ppns.ac.id

Imam Sutrisno is with Departement of Safety and Risk Engineering, Surabaya State Shipbuilding Polytechnic, Surabaya, 60111, Indonesia. imamsby01@yahoo.com

$$X = (m + m_x)\dot{u} - (m + m_y)v_m r - m x_G r^2 \quad (1)$$
$$Y = (m + m_y)\dot{v}_m - (m + m_x)ur - m x_G \dot{r} \quad (2)$$
$$N = (I_{zz} + J_{zz} + m x_G^2)\dot{r} - m x_G(\dot{v}_m + ur) \quad (3)$$

The left-hand side of equations (1) to (3), X, Y, and N, are expressed as.

$$X = X_H + X_P + X_R + X_A + X_T \quad (4)$$
$$Y = Y_H + Y_R + Y_A + Y_T \quad (5)$$
$$N = N_H + N_R + N_A + N_T \quad (6)$$

m represents the vessel's mass, while mx and my denote the added mass components along the x-axis and y-axis, respectively. u represents the ship's surge velocity, vm denotes lateral velocity, and r indicates yaw rate. xG represents the center of gravity of the vessel. IzG represents the ship's moment of inertia, while Jz denotes the added moment of inertia.

The forces acting on the ship's hull include the surge force (X), the lateral force (Y), and the yaw moment (N). Subscripts H, C, W, and T denote hull, current, wind, and tugs, respectively.

B. Hydrodynamic hull force and moment

The hull force and moment can be expressed as follows.

$$X_H = 0{,}5\rho L d U^2(-R'_0 + X'_{vv}v'm^2 + X'_{vr}v'_m r' + X'_{vvv}r'^2 + X'_{rrr}r'^4) \quad (4)$$
$$Y_H = 0{,}5\rho L d U^2(Y'_v v'_m + Y'_r r' + Y'_{vvv}v'^3_m + Y'_{vvr}v'^2_m r' + Y'_{vrr}v'_m r'^2 + Y'_{rrr}r'^3) \quad (5)$$
$$N_H = 0{,}5\rho L^2 d U^2(N'_v v'_m + N'_r r' + N'_{vvv}v'^3_m + N'_{vvr}v'^2_m r' + N'_{vrr}v'_m r'^2 + N'_{rrr}r'^3) \quad (6)$$

Where L,d, and U are the Length between perpendicular, the ship's draft, and the speed resultant, respectively. v'_m represents the non-dimensionalized lateral velocity defined by v_m/U, while r' non-dimensionalized yaw rate by $rLpp/U$.

C. Ships Resistance

To determine the ship's resistance using the Holtrop Method, expressed as.

$$R_{Total} = Rf(1 + k_1) + RAPP + RW + RB + RTR + RA \quad (7)$$

Where Rf denotes frictional resistance, $(1 + k_1)$ represent the form factor of the hull, RAPP indicates appendage resistance, RB refers to additional pressure resistance of the bulbous bow near the water surface, RTR represents additional pressure resistance caused by transom immersion, and RA denotes model-ship correlation resistance.

D. Determine Hydrodynamic Derivatives

Computational Fluid Dynamics analysis was conducted to obtain hydrodynamic coefficient values, where CFD provides the surge force (X), sway force (Y), and yaw moment (N). The CFD analysis was performed under two conditions:

1) Condition A: The ship is aligned parallel to the x-axis, and the simulation is performed using a straight flow domain.
2) Condition B: The ship is in a yawing position of 45 degrees with the rudder aligned parallel to the x-axis, and the simulation is performed using a circular flow domain.

Furthermore, hydrodynamic derivatives were also calculated using empirical formulas obtained from another research[13]. These two methods are preferred over model testing, because model testing spends more time and money[14].

3) *Wind Force and Moment*

Assessing the impact of wind on a ship's maneuvering performance is a crucial consideration [15]. Stronger winds need more power consumption[16]

$$X_A = \frac{1}{2}\rho_a V_A^2 A_T C_{XA}(\theta_A) \quad (7)$$
$$Y_A = \frac{1}{2}\rho_a V_A^2 A_L C_{YA}(\theta_A) f_A(\emptyset) \quad (8)$$
$$N_A = \frac{1}{2}\rho_a V_A^2 L A_L C_{NA}(\theta_A) f_A(\emptyset) \quad (9)$$

Where ρ_a denotes air density, A_T represents the transverse projected area, A_L signifies the lateral projected area. $C_{XA}, C_{YA}, and\ C_{NA}$ denote the aerodynamic force coefficients for surge, lateral, and yaw moments, respectively. θ_A denotes relative wind direction, f_A denotes the correction coefficient when the ship heels, and $\emptyset$ is roll angle. Va is the relative wind velocity calculated as follows.

$$V_A^2 = u_A^2 + vV_A^2 \quad (10)$$
$$u_A = u + U_W\cos(\theta_W - \psi) \quad (11)$$
$$v_A = v + U_W\sin(\theta_W - \psi) \quad (12)$$

U_W is absolute wind velocity, θ_W is the absolute wind direction, and ψ is ships heading[17].

4) *Tug Forces and Moment*

It is very important to accurately estimate the required tugboat pulling forces and the number of tugboats before berthing operations begin[18]. Tug forces and moment can be calculated as follows.

$$XT = F_T cos\Theta_T \quad (13)$$
$$YT = F_T sin\Theta_T \quad (14)$$
$$NT = Y_T(L/2) \quad (15)$$

F_T is the tug's force, Θ_T is the relative direction of the tug force, and L/2 denotes the arm of the tug moment.

5) *Current Effect*

Sea currents can significantly affect a ship's navigation[19]. The current effect can be calculated as follows.

TABLE 1.
SHIP PRINCIPAL DIMENSION

Main Principal	LOA	LPP	Beam (B)	Height (H)	Draught (T)	Speed (V)	Cb
Dimension	100.58 m	96.56 m	33.53 m	6.10 m	4.71 m	5 Knots	0.88

$$U = U_r = \sqrt{{u_r}^2 + {v_r}^2} \quad (16)$$

III. RESULTS AND DISCUSSION

A. Research Data

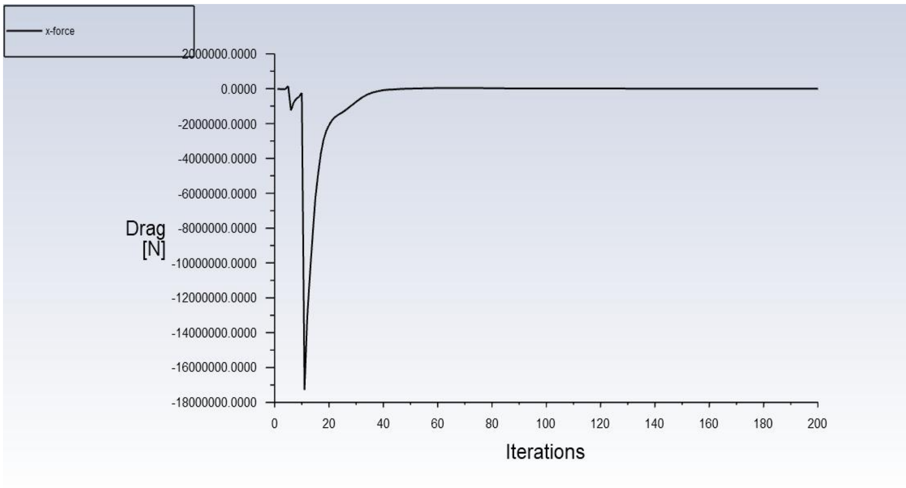

Figure. 1. The Force Value of X-axis (Straight Flow)

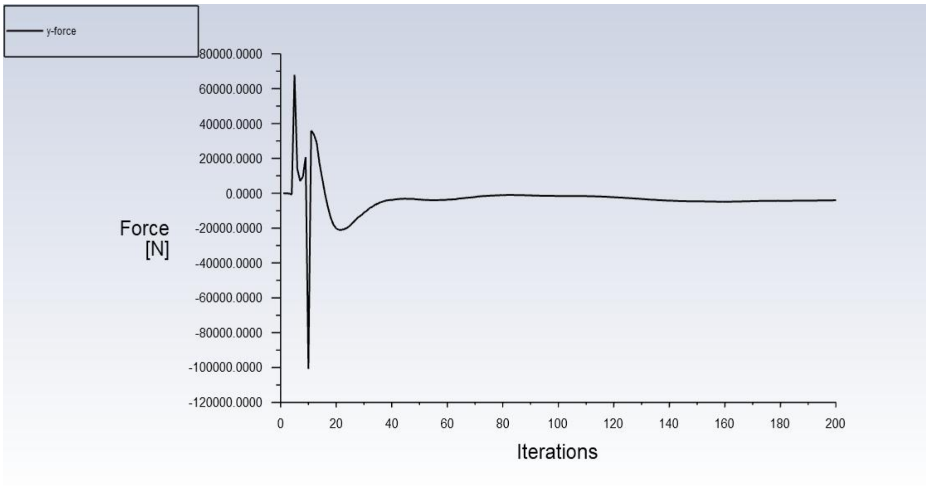

Figure. 2. The Force Value of Y-axis (Straight Flow)

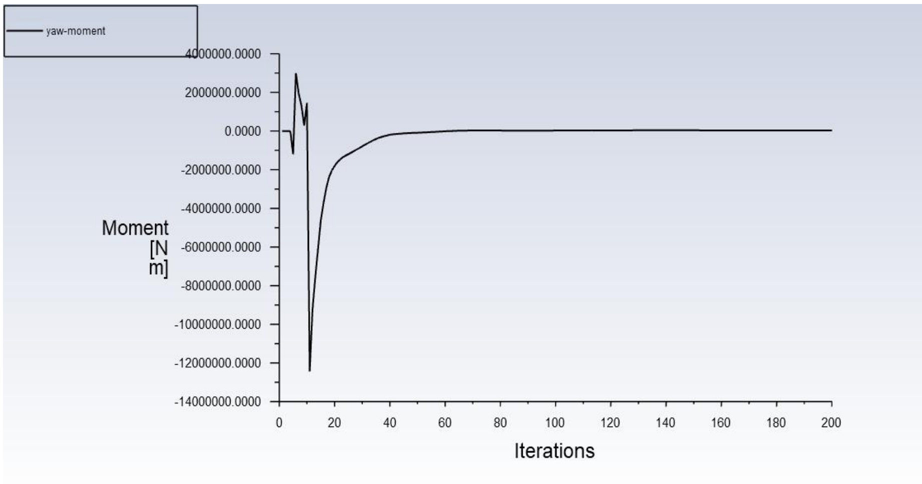

Figure. 3. The Yaw Moment Value (Straight Flow)

$$u = u_r = (u_b - u_c) = (u_b - U_c \cos \Psi_{c_r}) \quad (17)$$

$$v_m = v_r = (v_b - v_c) = (v_b - U_c \sin \Psi_{c_r}) \quad (18)$$

$$r = \Psi_{c_r} \, dan \, \Psi_{c_r} = \Psi - \Psi_c \quad (19)$$

The ship's body and the current are denoted with subscripts b and c, respectively.

The Ship's Principal Dimension can be seen in Table 1.

B. Computational Fluid Dynamics Analysis

Computational fluid dynamics for ship hydrodynamics has been developed significantly across various industries[20].

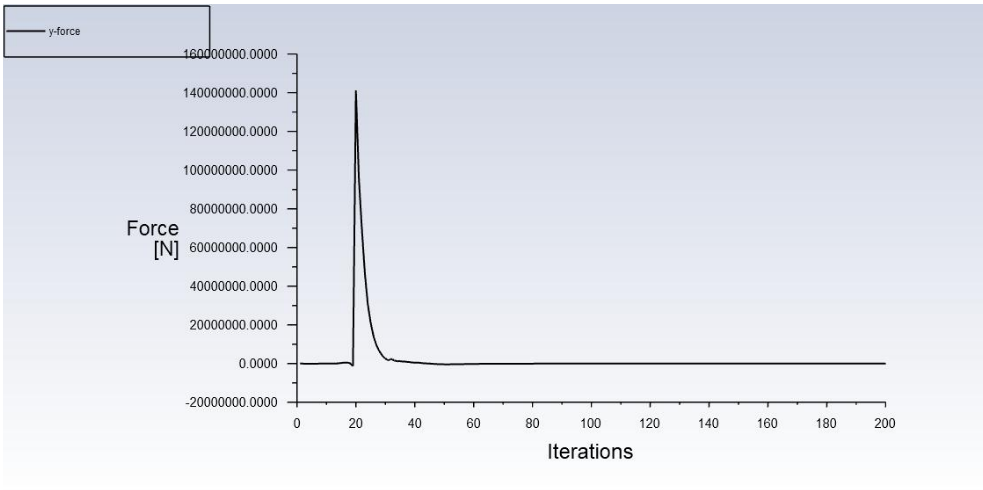

Figure. 4. The Force Value of y-axis (Circular Flow)

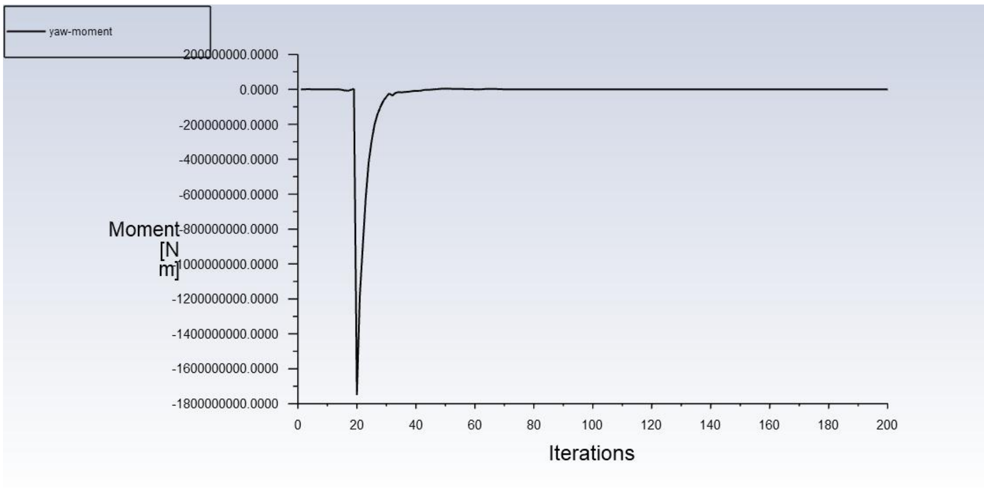

Figure. 5. The Yaw Moment Value (Circular Flow)

Several studies use CFD to predict Hydrodynamic derivatives. Kolodziej et. al. develop a computational approach to predict ship maneuverability by analyzing the hydrodynamic characteristics using CFD. Specifically, the study directly simulates circular motion tests (CMT) using CFD to obtain these characteristics[21]. CFD should be used to establish the berthing maneuver MMG model[22]. Several CFD-generated derivatives had replaced the empirical formulas[23].

The Straight Flow Domain and the Circular Flow Domain were visualized using Ansys Fluent in the Geometry section.

The output of the CFD analysis consists of the force values along the x-axis (surge), y-axis (sway), and the moment (yaw) acting on the hull. These values are converted into non-dimensional forms or derivatives for subsequent use in maneuverability analysis. Tables 3. and 4. show the force and moment obtained from CFD Analysis.

Figures .1 to 3 show the force and moment values derived from a straight flow domain. The force acting on the x-axis is 2554.3 N, and it is non-dimensionalized to 0.0526. The force acting on the y-axis is -4027,1 and non-dimensionalized to -0,0829. The yaw moment is 28670.8 N · m and non-dimensionalized to 0.0294.

Figure 4 and Figure 5. shows the force and moment values derived from a circular flow domain. The force acting on the y-axis is -9022.4 N and non-dimensionalized to -0.1858. The yaw moment is 64,920.8 N · m, and non-dimensionalized to 0.0665.

Hydrodynamic coefficients are obtained by dividing those above non-dimensional computational results by the non-dimensional lateral velocity (v′) for straight flow and the non-dimensional yaw rate (r′) for circular flow. The lateral velocity is derived from v = U sin β , where

TABLE 2.
HYDRODYNAMIC DERIVATIVES FROM CFD

Coefficient	X_v'	Y_v'	N_v'	Y_r'	N_r'
Value	0,0916	-0,1445	0,0511	-0,4157	0,1486

TABLE 5.
HYDRODYNAMIC DERIVATIVES

Coefficient	Value	References
Xvv’	-0.0706	Lee et.al. (1998)
Xvr’	-0.2797	Yoshimura et. al. (2012)
Xrr’	-0.0376	Lee et.al. (1998)
Xvvvv’	-0.8597	Yoshimura et. al. (2012)
Yv’	-0.1445	CFD
Yr’	-0.4157	CFD
Yvvv’	-0.1752	Lee et.al. (1998)
Yvvr’	-.04646	Lee et.al. (1998)
Yvrr’	-0.1003	Kijima et. al. (1990)
Yrrr’	0.6529	Lee et.al. (1998)
Nv’	0.0511	CFD
Nr’	0.1487	CFD
Nvvv’	0.5530	Lee et.al. (1998)
Nvvr’	-0.0516	Kijima et. al. (1990)
Nvrr’	0.0118	Kijima et. al. (1990)
Nrrr’	0.0173	Yoshimura et. al. (2012)

v' = v/U is the non-dimensional velocity. The non-dimensional yaw rate is obtained from r=U/R, with the non-dimensional r′=L/R, where L is the ship's length and R is the towing arm of the computational domain in Condition B. The results of hydrodynamic derivatives are presented in Table 2.

C. Determine Hydrodynamic Derivatives

Ensuring the navigational safety of a vessel entails the determination of the hydrodynamic derivatives, which is a very challenging one[24].

Table 3. presents the Hydrodynamic Derivatives obtained using CFD and the empirical method. These will be used to calculate the forces and moments acting on the ship's hull.

Kijima et al. presented a technique that facilitates the early-stage design of a ship's maneuverability by estimating the hydrodynamic forces acting on the ship under various loading conditions. These approximate formulas were derived from model test results. When compared with measured results from free-running model tests, the predictions using this formula show good agreement[25].

Yoshimura improved the accuracy of manoeuvring performance prediction for various merchant ships, especially considering large trim conditions. The authors achieve this by creating a new database of hydrodynamic coefficients and developing improved regression models to predict these coefficients. Ultimately, the goal is to provide a more reliable and practical prediction tool for ship designers at the early stages[26].

D. Ships Resistance

To determine the ship's resistance using the Holtrop Method, use equation (7). The result of the ship's resistance is shown in Table 4.

TABLE 3.
SHIPS RESISTANCE

Ship Speed (Knot)	6	5	4	3	2	1
Resistance (N)	508,217.83	44,092.73	29,080.33	16,993.66	7,967.32	7,967.32

TABLE 4.
PIANC REQUIREMENT OF SHIP’S BERTHING SPEED

Vessel Displacement (tons)	Favourable Condition (m/s)	Moderate Condition (m/s)	Unfavourable Condition (m/s)
Under 10,000	0.2 – 0,16	0.45 – 0.3	0.6 – 0.4
10,000 – 50,000	0.12 – 0.08	0.3 – 0.15	0.45 – 0.22
50,000 – 100,000	0.08	0.15	0.2
Over 100,000	0.08	0.15	0.2

TABLE 6.
ENVIROMENTAL CONDITION

Parameter	Condition 1	Condition 2	Condition 3
Current Speed (m/s)	0.44	0.31	0.58
Current Direction	West to East	East to West	East to West
Wind Speed (Knot)	5	5	10
Wind Direction	South East to North West	East to West	West to East

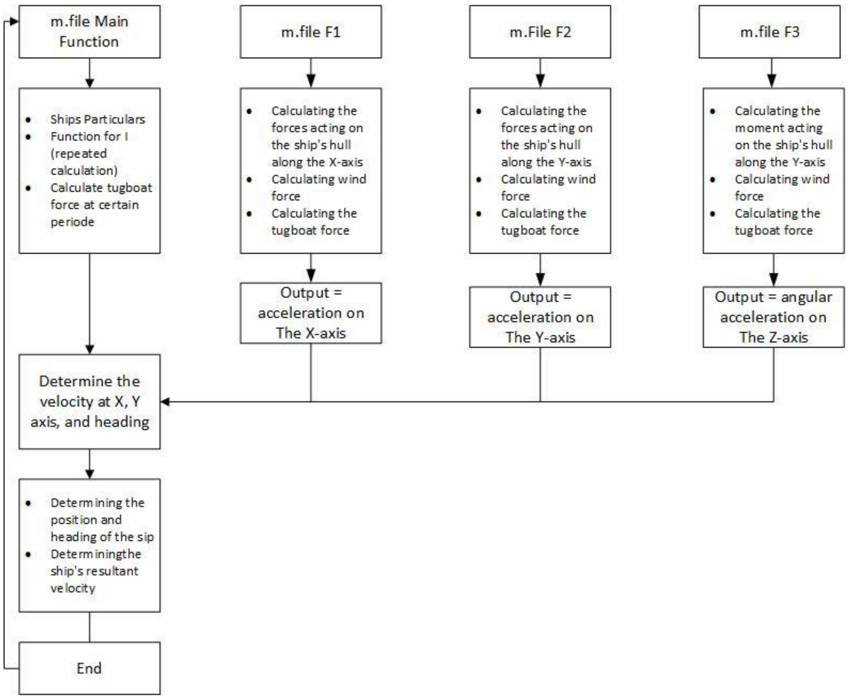

Figure. 6. MATLAB Simulation Flowchart

E. MATLAB Function

Wakita et. al. demonstrated that the neural network model accurately simulates low-speed maneuvering motions[27].

Figure 6. describes the MMG simulation flowchart. To perform simulations using the Maneuvering Modeling Group (MMG) in MATLAB, the initial step involves creating three separate m-files: F1, F2, and F3. The F1 m-file will contain the calculations for forces acting on the ship along the x-axis, F2 for forces along the y-axis, and F3 for the moment acting on the z-axis.

In developing the main function, it is crucial to identify which variables are constant and which can be adjusted. Subsequently, a for loop logic must be implemented to encompass the entire calculation process. This calculation begins by inputting values for current and wind. It then proceeds with the calculation of the tugboat force, which utilizes conditional (if) logic.

Following this, the functions from m-files F1, F2, and F3 will be called. The output from these function calls will be the acceleration along the x-axis, the acceleration along the y-axis, and the angular acceleration around the z-axis. Using these accelerations, the values for velocity components (u, v), yaw rate (r), and heading for the next iteration (i+1) can be determined. These values of u, v, r, and heading at iteration i+1 will then be used back in the main function for the looping calculation.

F. Acceptance Criteria of Berthing Speed

The berthing velocity should be considered size of the ship[28]. Mwange et. al. reveal that speed reduction significantly improves berthing safety[29].

Based on PIANC's requirements, vessels with a displacement of 10.000 to 50,000 tons are permitted to berth at a maximum velocity of 0.3 m/s, as detailed in Table 5[30].

G. MMG Simulation

Mitsuyuki et al. reveal that the precision of trajectory prediction with mathematical models of ship maneuverability is a crucial technology employed in autonomous surface vessels. However, real-world operational conditions are not always ideal. Ships in the real world do not operate in perfect accordance with a complete ship maneuverability mathematical model[31]. Considering environmental disturbances ensures that ship maneuvering predictions are more accurate, realistic, and safely applicable in dynamic real-world operational conditions.

Ship berthing is a challenging task due to factors such as changes in dynamic characteristics in narrow waterways, the lack of controllability of large merchant

TABLE 7.
THE RESULT OF MMG SIMULATION

Scenario	Wind Speed (Knots)	Wind Direction	Current Speed (m/s)	Current Direction	Initial Speed (Knots)	Initial Heading (Degree)	Berthing		PIANC Acceptance Criteria
							Knots	m/s	
1.	5	135 (SW to NW)	0,44	90 (W to E)	0	210	0,278	0,143	Moderate
2.					2	195	0,455	0,234	Moderate
3.					2,9	189	0,219	0,113	Favourable
4.					4	196	0,281	0,145	Moderate
5.					5	196	0,587	0,302	Unfavourable
6.	5	315 (NW to SW)	0,31	270 (E to W)	0	152	0,271	0,139	Moderate
7.					2	158	0,496	0,255	Moderate
8.					2,9	158	0,132	0,068	Favourable
9.					4	165	0,474	0,244	Moderate
10.					5	166	0,494	0,254	Moderate
11.	10	270 (W to E)	0,58	270 (E to W)	0	139	0,059	0,030	Favourable
12.					2	150	0,320	0,165	Moderate
13.					2,9	152	0,489	0,252	Moderate
14.					4	158	0,420	0,216	Moderate
15.					5	165	0,478	0,246	Moderate

ships at low speeds, and unpredictable environmental disturbances.

Moreover, Okuda et al. demonstrate that the 4-DOF MMG approach yields accurate simulation results that align with the free-running test findings, demonstrating a high level of practical precision[32]. As a result, the 4-DOF MMG approach facilitates the prediction of maneuvering for fast ships.

Ship berthing is a challenging task due to factors such as changes in dynamic characteristics in narrow waterways, the lack of controllability of large merchant ships at low speeds, and unpredictable environmental disturbances[33].

In this simulation, there will be three environmental conditions. The data were obtained from the Indonesian Meteorology, Climatology, and Geophysics Agency during a specific period. This data will serve as input for the MMG simulation, as shown in Table 6. The MMG simulations conducted under three distinct environmental conditions (variations in wind speed and direction, as well as current speed and direction) reinforce the understanding that external factors have a significant impact on ship maneuvering. Despite the varied environmental conditions, the findings consistently show that the 4-knot limit remains a safe threshold. This illustrates the value of carefully considering local environmental dynamics in operational planning. The research results suggest that, although environmental conditions can exacerbate maneuvering challenges, adhering to the recommended initial speed limit can effectively mitigate associated risks.

This simulation assumes that a 30,000-ton bollard pull tugboat pulls the barge. There are three environmental conditions, each with five initial speed variations, resulting in a total of 15 scenarios.

Table 7. shows the result of the MMG simulation. Scenario 5 (Environmental Condition 1) is the most critical. With an initial speed of 5 knots, even though the wind speed (5 knots) and current speed (0.44 m/s) are not the most extreme compared to Condition 3, the combination of wind direction (southwest to northwest) and current direction (west to east) resulted in a final berthing speed of 0.302 m/s, which is categorised as unfavourable. This indicates that not only the magnitude of the disturbance but also its relative direction to the ship's maneuver and berthing path is significant. Wind and current in specific directions can create forces and moments that exacerbate the tugboat's efforts to control the ship's speed and position.

Scenarios 10 and 15 (Environmental Conditions 2 and 3 at 5 knots). Despite having the same initial speed (5 knots), their final berthing speeds (0.254 m/s and 0.246 m/s) still fall within the moderate criteria. Environmental Condition 2 has a lower current speed (0.31 m/s) compared to Conditions 1 and 3. Environmental Condition 3 has the highest wind and current speeds (wind 10 knots, current 0.58 m/s). However, the fact that the results are still moderate, although approaching the upper limit, suggests that the wind direction (west to east) and current direction (east to west) in this scenario may slightly assist in naturally slowing the vessel as it approaches the berth or minimize transverse forces that cause uncontrolled movement. This emphasizes that the dynamic nature and complex interactions of environmental disturbances must be carefully evaluated.

One of the most significant findings is the identification that an initial speed of 5 knots consistently results in a berthing simulation categorized as unfavourable according to PIANC standards. This directly indicates that at this speed, the risk of collision with the jetty increases drastically. Conversely, the simulations demonstrated that initial speeds below 5 knots, particularly up to 2.9 knots, consistently yielded safe final berthing speeds below 0.3 m/s and met PIANC's Favourable to Moderate criteria.

IV. CONCLUSION

The MMG simulation results indicate that at an initial speed of 5 knots, the berthing condition is categorized as unfavourable according to PIANC standards. This suggests an increased risk of collision with the jetty at that speed. Conversely, the simulations confirm that at initial speeds below 5 knots, the barge can be safely berthed. Specifically, the final berthing speeds consistently remained below 0.3 m/s or were categorized as favourable to moderate, provided that specific tugboat power percentages and maneuvering strategies were employed.

This research concludes that the maximum acceptable initial speed of a tugboat at Paciran Port, to avoid collision with the jetty during tugboat-assisted berthing, is below 4 knots. Establishing this speed limit is crucial for enhancing operational safety and reducing the potential for incidents at Paciran Port.

REFERENCES

[1] G. Hejun, F. Fuquan, J. Xiaobin, W. Deling, and T. Qingfeng, "Ship Berthing Safety Assessment Based on Ship-Handling Simulator," *American Journal of Traffic and Transportation Engineering*, vol. 6, no. 1, p. 10, 2021, doi: 10.11648/j.ajtte.20210601.12.

[2] J. Mentjes, H. Wiards, and S. Feuerstack, "Berthing Assistant System Using Reference Points," *J Mar Sci Eng*, vol. 10, no. 3, p. 385, Mar. 2022, doi: 10.3390/jmse10030385.

[3] R. M. Darbra, J. F. E. Crawford, C. W. Haley, and R. J. Morrison, "Safety culture and hazard risk perception of Australian and New Zealand maritime pilots," *Mar Policy*, vol. 31, no. 6, pp. 736–745, Nov. 2007, doi: 10.1016/j.marpol.2007.02.004.

[4] G. Taimuri, J. Matusiak, T. Mikkola, P. Kujala, and S. Hirdaris, "A 6-DoF maneuvering model for the rapid estimation of hydrodynamic actions in deep and shallow waters," *Ocean Engineering*, vol. 218, p. 108103, Dec. 2020, doi: 10.1016/j.oceaneng.2020.108103.

[5] G. Go and H. T. Ahn, "Hydrodynamic derivative determination based on CFD and motion simulation for a tow-fish," *Applied Ocean Research*, vol. 82, pp. 191–209, Jan. 2019, doi: 10.1016/j.apor.2018.10.023.

[6] B. Zhao, X. Zhang, and C. Liang, "A Novel Parameter Identification Algorithm for 3-DOF Ship Maneuvering Modelling Using Nonlinear Multi-Innovation," *J Mar Sci Eng*, vol. 10, no. 5, p. 581, Apr. 2022, doi: 10.3390/jmse10050581.

[7] A. H. Muhammad, . Syarifuddin, D. Paroka, S. Rahman, . Wisyono, and A. A. Pratama, "MANEUVERING PERFORMANCE OF A 30 GT FISHING VESSEL WITH ASYMMERICAL PROPELLER CONFIGURATION," *Jurnal Ilmu dan Teknologi Kelautan Tropis*, vol. 9, no. 2, pp. 491–498, Jan. 2018, doi: 10.29244/jitkt.v9i2.19314.

[8] Y. Xia, S. Zheng, Y. Yang, and Z. Qu, "Ship Maneuvering Performance Prediction Based on MMG Model," *IOP Conf Ser Mater Sci Eng*, vol. 452, p. 042046, Dec. 2018, doi: 10.1088/1757-899X/452/4/042046.

[9] M. , & H. K. Sano, "A fundamental study on the ship handling simulation of tug–barge and pusher–barge systems for river service," *ICSOT India: Coastal & Inland Shipping*, 2015.

[10] IPS. Asmara, E. Kobayashi, and T. Pitana, "Simulation of Collision Avoidance by Considering Potential Area of Water for Maneuvering based on MMG Model and AIS Data," in *Proceedings of the 3rd International Conference on Simulation and Modeling Methodologies, Technologies and Applications*, SciTePress - Science and and Technology Publications, 2013, pp. 243–250. doi: 10.5220/0004478002430250.

[11] I. Asmara and A. W. Husodo, "Ship to Ship Manoeuvring Simulation to Determine Elements of Tugboat Handling," *IOP Conf Ser Earth Environ Sci*, vol. 1081, no. 1, p. 012014, Sep. 2022, doi: 10.1088/1755-1315/1081/1/012014.

[12] H. Yasukawa and Y. Yoshimura, "Introduction of MMG standard method for ship maneuvering predictions," *J Mar Sci Technol*, vol. 20, no. 1, pp. 37–52, Mar. 2015, doi: 10.1007/s00773-014-0293-y.

[13] O. F. Sukas, O. K. Kinaci, and S. Bal, "Theoretical background and application of MANSIM for ship maneuvering simulations," *Ocean Engineering*, vol. 192, p. 106239, Nov. 2019, doi: 10.1016/j.oceaneng.2019.106239.

[14] S.-H. Kim, C.-K. Lee, and S.-M. Lee, "Estimation of Maneuverability of Fishing Vessel Considering Hull-Form Characteristics," *J Mar Sci Eng*, vol. 9, no. 6, p. 569, May 2021, doi: 10.3390/jmse9060569.

[15] H. Yasukawa and R. Sakuno, "Application of the MMG method for the prediction of steady sailing condition and course stability of a ship under external disturbances," *J Mar Sci Technol*, vol. 25, no. 1, pp. 196–220, Mar. 2020, doi: 10.1007/s00773-019-00641-4.

[16] E. Kløvning, "Wind Affecting Berthing Operations," *TransNav, the International Journal on Marine Navigation and Safety of Sea Transportation*, vol. 14, no. 3, pp. 721–725, 2020, doi: 10.12716/1001.14.03.26.

[17] T. Fujiwara, M. Ueno, and T. Nimura, "Estimation of Wind Forces and Moments acting on Ships," *Journal of the Society of Naval Architects of Japan*, vol. 1998, no. 183, pp. 77–90, 1998, doi: 10.2534/jjasnaoe1968.1998.77.

[18] V. Paulauskas and D. Paulauskas, "Ship Mooring Methodology Designed for Ship Berthing in Extremely Limited Conditions," *J Mar Sci Eng*, vol. 13, no. 3, p. 575, Mar. 2025, doi: 10.3390/jmse13030575.

[19] C. Chen, S. Shiotani, and K. Sasa, "Effect of ocean currents on ship navigation in the east China sea," *Ocean Engineering*, vol. 104, pp. 283–293, Aug. 2015, doi: 10.1016/j.oceaneng.2015.04.062.

[20] N. Degiuli and I. Martić, "CFD Applications in Ship and Offshore Hydrodynamics," *J Mar Sci Eng*, vol. 12, no. 11, p. 1926, Oct. 2024, doi: 10.3390/jmse12111926.

[21] R. , & H. P. Kołodziej, "Numerical Estimation Of Hull Hydrodynamic Derivatives In Ship Maneuvering Prediction ," *POLISH MARITIME RESEARCH*, vol. 28, no. 2, pp. 46–53, 2021.

[22] S. Zhang, Q. Wu, J. Liu, Y. He, and S. Li, "State-of-the-Art Review and Future Perspectives on Maneuvering Modeling for Automatic Ship Berthing," *J Mar Sci Eng*, vol. 11, no. 9, p. 1824, Sep. 2023, doi: 10.3390/jmse11091824.

[23] S. He, P. Kellett, Z. Yuan, A. Incecik, O. Turan, and E. Boulougouris, "Manoeuvring prediction based on CFD generated derivatives," *Journal of Hydrodynamics*, vol. 28, no. 2, pp. 284–292, Apr. 2016, doi: 10.1016/S1001-6058(16)60630-3.

[24] S. Janardhanan and P. Krishnankutty, "Determination of Linear and Non-linear Hydrodynamic Derivatives of a Surface Ship in Manoeuvring Using CFD Method," 2020, pp. 95–121. doi: 10.1007/978-981-13-9806-3_4.

[25] K. , K. T. , N. Y. , & F. Y. Kijima, "On the manoeuvring performance of a ship with the parameter of loading condition," *Autumn Meeting of the Society of Naval Architects of Japan*, 1990.

[26] Y. , & M. Y. (2011). Yoshimura, "Hydrodynamic Force Database with Medium High Speed Merchant Ships Including Fishing Vessels and Investigation into a Maneuvering Prediction Method," *Journal of Japan Society of Naval Architects and Ocean Engineers*, vol. 14, pp. 63–73, 2011.

[27] K. Wakita *et al.*, "On neural network identification for low-speed ship maneuvering model," *J Mar Sci Technol*, vol. 27, no. 1, pp. 772–785, Mar. 2022, doi: 10.1007/s00773-021-00867-1.

[28] H.-T. Lee, S.-W. Lee, J.-W. Cho, and I.-S. Cho, "Analysis of Feature Importance of Ship's Berthing Velocity Using Classification Algorithms of Machine Learning," *Journal of the Korean Society of Marine Environment and Safety*, vol. 26, no. 2, pp. 139–148, Apr. 2020, doi: 10.7837/kosomes.2020.26.2.139.

[29] A. N. Mwange, D. M. Rachman, R. Suyama, and A. Maki, "A practical and online trajectory planner for autonomous ships' berthing, incorporating speed control," *J Mar Sci*

Technol, vol. 30, no. 1, pp. 238–254, Mar. 2025, doi: 10.1007/s00773-025-01048-0.

[30] A. A. Roubos, R.; Williams, and P. Mirihagalla, “Recommendations for berthing velocity in PIANC WG211,” in *Proceedings of the 35th PIANC World Congres 2024*, 2024, pp. 1050–1056.

[31] T. Mitsuyuki *et al.*, “MMG 3DOF model identification with uncertainty of observation and hydrodynamic maneuvering coefficients using MCMC method,” *J Mar Sci Technol*, vol. 29, no. 3, pp. 668–682, Sep. 2024, doi: 10.1007/s00773-024-01013-3.

[32] R. Okuda, H. Yasukawa, and A. Matsuda, “Validation of maneuvering simulations for a KCS at different forward speeds using the 4-DOF MMG method,” *Ocean Engineering*, vol. 284, p. 115174, Sep. 2023, doi: 10.1016/j.oceaneng.2023.115174.

[33] J.-H. Choi, J.-Y. Jang, and J. Woo, “A Review of Autonomous Tugboat Operations for Efficient and Safe Ship Berthing,” *J Mar Sci Eng*, vol. 11, no. 6, p. 1155, May 2023, doi: 10.3390/jmse11061155.